Available online at www.sciencedirect.com

SciVerse ScienceDirect

Ceramics International 39 (2013) S421–S426

CERAMICS INTERNATIONAL

www.elsevier.com/locate/ceramint

The effects of sintering temperature and content of x on phase formation, microstructure and dielectric properties of $(1-x)(Bi_{0.4871}Na_{0.4871}La_{0.0172}TiO_3)-x(BaZr_{0.05}Ti_{0.95}O_3)$ ceramics prepared via the combustion technique

Chittakorn Kornphom[a,b], Artid Laowanidwatana[a,b], Theerachai Bongkarn[a,b,*]

[a]*Department of Physics, Faculty of Science, Naresuan University, Phitsanulok 65000, Thailand*
[b]*Research Center for Academic Excellent in Petroleum, Petrochemicals and Advanced Materials, Naresuan University, Phitsanulok 65000, Thailand*

Available online 24 October 2012

Abstract

$(1-x)(Bi_{0.4871}Na_{0.4871}La_{0.0172}TiO_3)-x(BaZr_{0.05}Ti_{0.95}O_3)$ ceramics (abbreviated $(1-x)$BNLT$-x$BZT) where $0.1 \le x \le 0.3$ were fabricated by the combustion technique using glycine as fuel. BNLT and BZT powders were calcined at temperatures of 825 °C for 4 h and 925 °C for 6 h, respectively. After that they were mixed with the different compositions. It was found that the optimum sintering temperature of $(1-x)$BNLT$-x$BZT ceramic was obtained at 1125 °C for 2 h. This ceramic had the highest density. The structure of the $(1-x)$BNLT$-x$BZT ceramics exhibited the co-existence of tetragonal and rhombohedral phases with $x \le 0.1$. The tetragonality increases with the increase of x content. The average grain size, the density and the Curie temperatures decrease with increasing x content. The maximum dielectric constant and the highest P_r were at about 4850 and 12.7 μC/cm^2, respectively, and were obtained by the 0.85BNLT$-$0.15BZT sample.
© 2012 Elsevier Ltd and Techna Group S.r.l. All rights reserved.

Keywords: Sintering; Ferroelectric properties; Dielectric properties; Perovskites

1. Introduction

$Bi_{0.4871}Na_{0.4871}La_{0.0172}TiO_3$ (abbreviated as BNLT) is a kind of lead-free piezoelectric material which is a ferroelectric with a rhombohedral perovskite structure at room temperature [1]. BNLT ceramic exhibits a good dielectric constant at room temperature (515) [1] and a high piezoelectric coefficient d_{33} (120 pC/N) [1]. Consequently, this ceramic is appropriate for application as the sensors, actuators and transducers [2]. $Ba(Zr_{0.05}TiO_{0.95})O_3$ ceramic (abbreviated as BZT) is one of the most studied piezoelectric materials due to its great piezoelectric properties (236 pC/N) with an orthorhombic perovskite structure at room temperature. It also exhibits a high dielectric constant (14,000) and low loss characteristic (0.05) at Curie temperature of 120 °C [3]. This ceramic has became widely attractive for use as multilayer ceramics capacitors and piezoelectric sensors/actuators [2].

To improve the electrical properties of lead-free piezoelectric materials, a new system of $(1-x)Bi_{0.4871}Na_{0.4871}La_{0.0172}TiO_3$–$xBaZr_{0.05}Ti_{0.95}O_3$ ($(1-x)$BNLT$-x$BZT) at a composition of around $0 \le x \le 1$ step 0.2 was proposed by Kantha et al. [3]. The $(1-x)$BNLT$-x$BZT ceramics were prepared by a two step mixed oxide method for synthesized the BNLT and BZT powders then sintered at temperatures between 1125 and 1400 °C for 2 h. The structure of the $(1-x)$BNLT–xBZT ceramics changed from a rhombohedral phase to a tetragonal phase when ≥ 0.2. For the $(1-x)$BNLT–xBZT ceramic $x \le 0.2$, the dielectric permittivity (ε_r) curve exhibited two peaks. The first curve was the phase transition temperature (T_p), corresponding to a ferroelectric rhombohrdral phase which transformed into a ferroelectric tetragonal phase.

*Corresponding author at: Department of Physics, Faculty of Science, Naresuan University, Phitsanulok 65000, Thailand. Tel.: +66 5596 3528; fax: +66 5596 3501.
E-mail address: researchcmu@yahoo.com (T. Bongkarn).

0272-8842/$ - see front matter © 2012 Elsevier Ltd and Techna Group S.r.l. All rights reserved.
http://dx.doi.org/10.1016/j.ceramint.2012.10.106

The second curve is Curie temperature (T_c) and it is related to the transition from a ferroelectric tetragonal phase to a paraelectric cubic phase [3]. A broad dielectric peak was observed to increase from the ε_r curves with x content ≥ 0.4. The ε_r measured at room temperature increased from 675 to 1575 with the increased of x content from 0 to 0.2. Upon further increasing x, the ε_r decreased. Appropriate ferroelectric properties is observed in the composition of $x=0.2$. Many changes in the phase formation, phase transition and electrical properties of $(1-x)$BNLT–xBZT ceramics were observed at around the composition of $x=0.2$.

In recent years, our previous work has successfully fabricated lead-free ferroelectric ceramics such as: (Bi Na)TiO_3 [4], $BaTiO_3$ [5], $BaZrO_3$ [6], Ba(Ti Zr)O_3 [7], (Bi Na)TiO_3–(Bi K)TiO_3 [4] via the combustion technique. The technique is simple. It has a low cost and it produces high quality ultra fine powders [8]. The ceramics fabricated by this technique possesses a high density and has good electrical properties [4–8]. Therefore, in the present work, the fabrication of the $(1-x)$BNLT–xBZT ceramics were prepared by the combustion technique, where a range of x values was chosen between 0.1 and 0.3 (mole step 0.05 was performed). The effects of sintering temperature on phase formation, microstructure of BNLT–BZT ceramics were investigated. The influence of x content on the crystal structure and the microstructure were studied. Special emphasis was focused on phase formation and the electrical properties of the composition between the BNLT and BZT systems in order to enhance these ceramics.

2. Experimental

The sample, $(1-x)(Bi_{0.4871}Na_{0.4871}La_{0.0172}TiO_3)-x(BaZr_{0.05}Ti_{0.95}O_3)$, (abbreviated as $(1-x)$BNLT$-x$BZT) where $0.1 \leq x \leq 0.3$, was prepared by the combustion technique using glycine as fuel. To synthesize $Bi_{0.4871}Na_{0.4871}La_{0.0172}TiO_3$ (BNLT) powder, reagent grade oxide and carbonate powders of Bi_2O_3 (99%), Na_2CO_3 (99%), La_2O_3 (99%) and TiO_2 (99%) were used as starting materials. The compositions of the raw materials were weighed and mixed by a ball-milling method for 24 h in absolute ethanol. The mixed powder was dried and ground using an agate mortar and then sieved into a fine powders. The mixed powder and glycine were mixed with a ratio of 1:2 in an agate mortar and calcined at 825 °C for 4 h. To synthesize the $BaZr_{0.05}Ti_{0.95}O_3$ (BZT) powder; $BaCO_3$ (99%), ZrO_2 (99%) and TiO_2 (99%) were used as raw materials. The processing of the BZT was similar to that of the BNLT powders but the uncalcined BZT powders were calcined at the temperatures of 925 °C for 6 h. The two calcined powders were a mixture of different compositions ($0.1 \leq x \leq 0.3$) and reground by the ball-milling method for 24 h. The mixtures were dried and sieved and then were made into pellets 15 mm in diameter using uniaxial pressing in a stainless steel mold. The pellets were sintered between 1050 °C and 1200 °C in an electric furnace at air atmosphere under controlled heating and a cooling rate of 5 °C/min with a soak time of 2 h. X-ray diffraction (XRD) was employed to identify the phase formed and the optimum temperature for $(1-x)$BNLT$-x$BZT ceramics. The sintered ceramics morphologies were imaged using scanning electron microscopy (SEM). The density of the sintered ceramics was measured by the Archimedes method. The average grain size was determined by a mean linear intercept method. The dielectric constant was observed by a LCR meter. The ferroelectric hysteresis (P–E) loops were characterized by using a computer controlled modified Sawyer–Tower circuit.

3. Results and discussion

The X-ray diffraction patterns of the 0.8BNLT–0.2BZT ceramics sintered at 1050–1200 °C for 2 h are shown in Fig. 1. All patterns of the sintered samples exhibited the tetragonal perovskite phase which matched with JCPDS file no. 03-0725 below 1200 °C. At the sintered temperature of 1200 °C, the second phase of $Bi_2Ti_2O_7$ occurred. This result may be caused by the evaporation of Na_2O and Bi_2O_3, which has a low melting point [9].

The SEM micrographs of the 0.8BNLT–0.2BZT ceramic surface sintered between 1100 and 1200 °C are presented in Fig. 2. The grain morphology exhibited an almost spherical morphology at low sintering temperature and changes to a polygonal morphology when the sintering temperature increased. At a low sintering temperature (below 1100 °C), the ceramics contained small and loosely bonded grains (Fig. 2(a)). The grain size increased and the porosity decreased when the sample was sintered at temperatures higher than 1100 °C (Fig. 2(b) and (c)). At a sintering temperature of 1200 °C, the ceramic exhibited a rugged surface and the a high porosity, as shown in Fig. 2(d). The

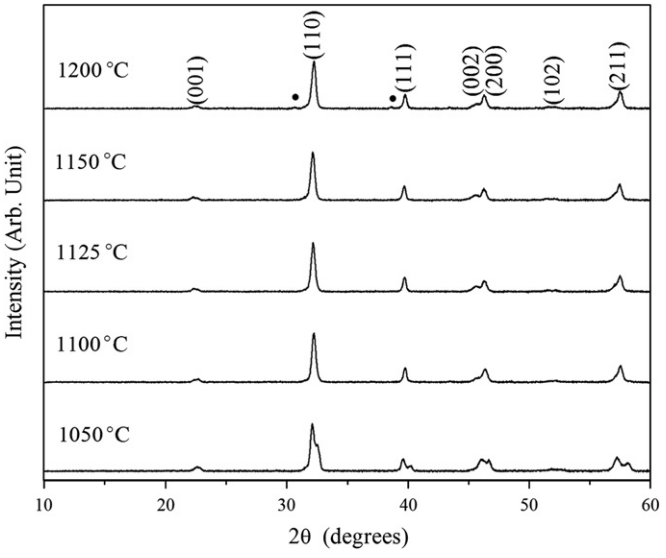

Fig. 1. XRD patterns of 0.8BNLT–0.2BZT ceramics sintered at various temperatures; (●) $Bi_2Ti_2O_7$.

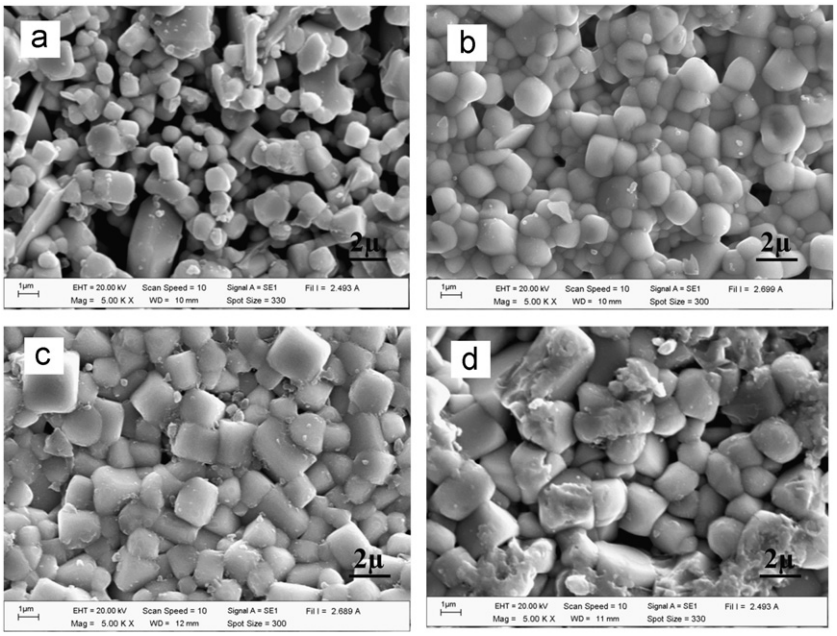

Fig. 2. The SEM micrographs of 0.8BNLT–0.2BZT surface pellet sintered at: (a) 1100, (b) 1125, (c) 1150 and (d) 1200 °C for 2 h.

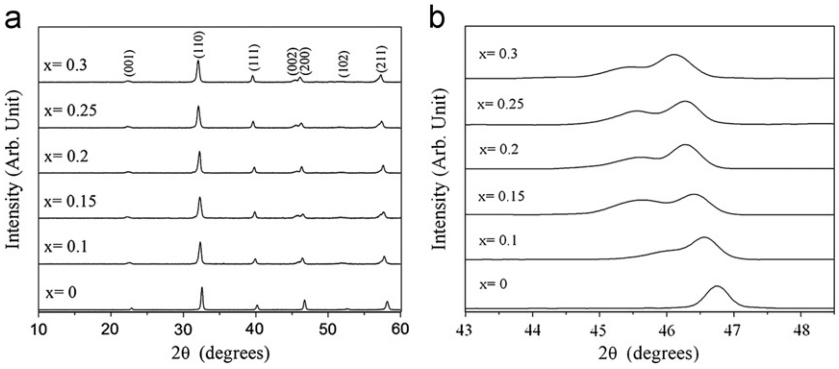

Fig. 3. XRD patterns of $(1-x)$BNLT–xBZT powders where $0.1 \leq x \leq 0.3$ sintered at 1125 °C for 2 h: (a) at high scanning rate and (b) at very low scanning rate.

occurrence of a rugged surface and a high porosity at high sintering temperatures indicated that the grain began to melt. This was caused by the evaporation of Na_2O and Bi_2O_3 at high sintering temperatures [9]. The microstructure is consistent with the XRD results. The average grain size increased from 0.48 to 1.33 μm when sintering temperature increased from 1100 °C to 1200 °C. The density of the 0.8BNLT–0.2BZT ceramics was increased from 5.57 to 5.79 g/cm^3 when the sintering temperatures increased up to 1125 °C, whereas the density decreased. The density results were consistent with a microstructure investigation. The optimum conditions for 0.8BNLT–0.2BZT was obtained at a sintering temperature of 1125 °C for 2 h.

To study the effect of x content on phase formation, microstructure and dielectric properties of $(1-x)(Bi_{0.4871}Na_{0.4871}La_{0.0172}TiO_3)-x(BaZr_{0.05}Ti_{0.95}O_3)$ ceramics, the two powders were mixed in ratios of $0.1 \leq x \leq 0.3$ and then made into pellets and sintered at 1125 °C for 2 h. The X-ray results of $(1-x)$BNLT$-x$BZT with $0.1 \leq x \leq 0.3$ are shown Fig. 3. All the samples exhibited the single perovskite phase (Fig. 3(a)).

The X-ray diffraction patterns of these ceramics also showed a phase change from rhombohedral to tetragonal, with increasing x content. The difference between these two structures can be seen clearly from Fig. 3(b) which represents the X-ray peaks at 2θ range between 43° and 48° that measured using a low scanning rate. The peak of (2 0 0) is observed in the diffraction pattern for pure BNLT, indicating that this is rhombohedral structures. When adding BZT of $0.1 \leq x \leq 0.3$, the peak of (2 0 0) split into two peaks of (0 0 2)/(2 0 0) and the peaks shifted slightly toward low angles. The peak of ceramics for $x=0.1$ is slightly asymmetrical, featured with inappreciable split of the (2 0 0) and (0 0 2) peaks, indicating the coexistence structures between rhombohedral and tetragonal phases. Doping of $x \geq 0.15$ leads to the apparent separation between (2 0 0) and (0 0 2) peaks, indicating an increase in the tetragonality of the ceramics. In the district

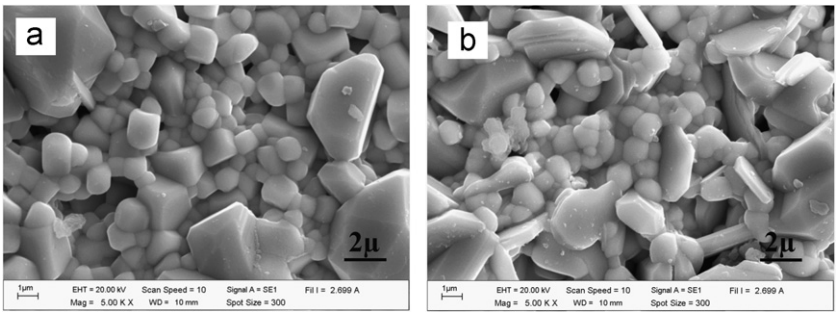

Fig. 4. The SEM micrographs of $(1-x)$BNLT–xBZT ceramics where x=(a) 0.1 and (b) 0.3 sintered at 1125 °C for 2 h.

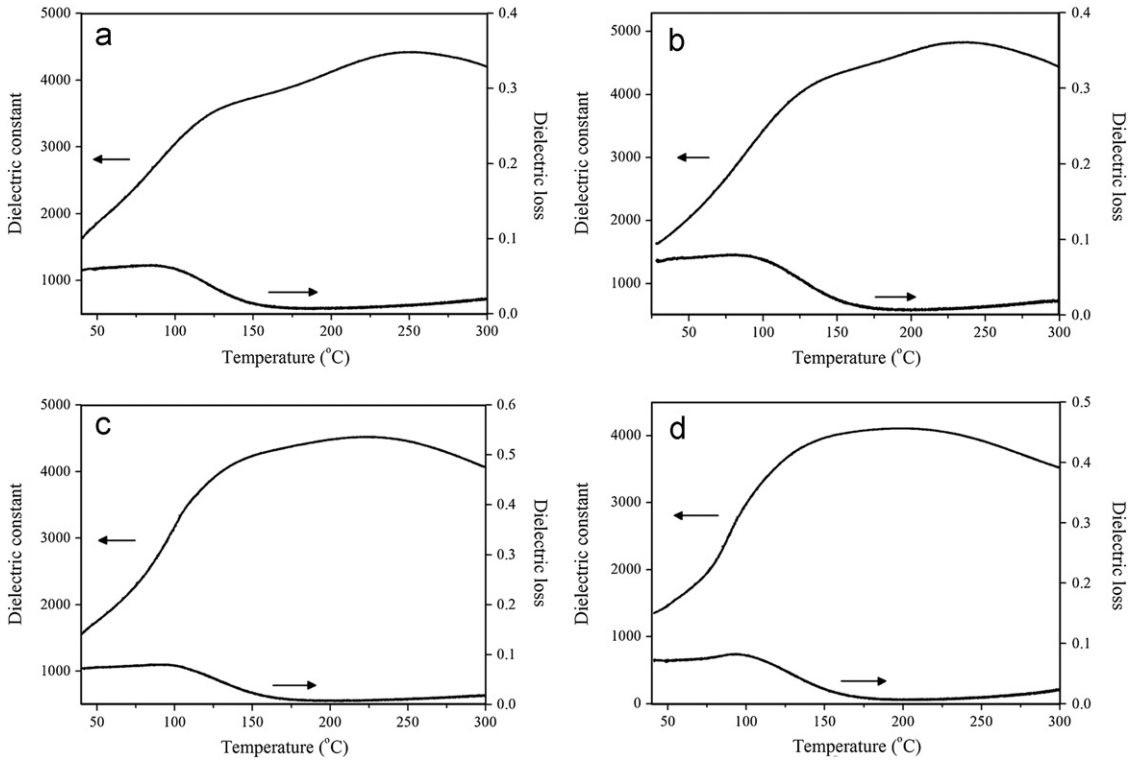

Fig. 5. Temperature dependence of dielectric constant and dielectric loss of $(1-x)$BNLT–xBZT sintered at 1125 °C for 2 h where x=(a) 0.1 (b) 0.15, (c) 0.2 and (d) 0.25.

of the tetragonal structure, the lattice parameters a and c of the $(1-x)$BNLT$-x$BZT system are listed in Table 1. The lattice parameters a and c increased gradually with increasing x content. The c/a ratio increased with increasing x up to 0.2, and then it decreased (Table 1).

Fig. 4 illustrates the SEM photomicrograph of $(1-x)$BNLT$-x$BZT ceramics with x=0.1 and 0.3 (Fig. 4(a) and (b)). It can be observed that the grain morphology of the ceramics exhibited an almost spherical morphology combined with a polygonal morphology. The porosity was found on the surface of all the samples. The porosity increased while the grain size decreased when the content of x increased (Table 1). The reduction in grain

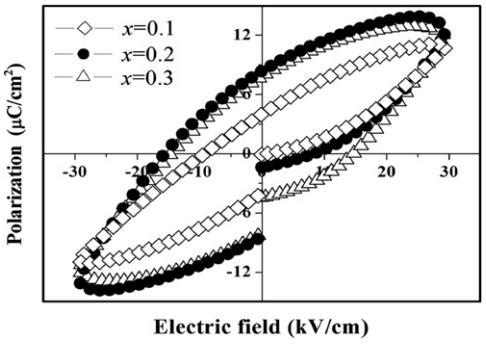

Fig. 6. P–E hysteresis loops of $(1-x)$BNLT–xBZT ceramics measured at electric field of 30 kV.

Table 1
Lattice parameters, c/a, average grain size, density, T_p, T_c, dielectric properties and ferroelectric properties of $(1-x)$BNLT–xBZT ceramics.

x	Lattice Parameters (Å)		c/a	Average grain size (μm)	Density (g/cm^3)	T_p (°C)	T_c (°C)	ε_r at T_p	tan δ at T_p	ε_r at T_c	tan δ at T_c	γ	P_r (μC/cm^2)	E_c (kV/cm)
	a	c												
0.1	3.913	3.956	1.0109	1.67	5.82	124	250	3630	0.036	4425	0.0011	1.61	8.3	16.1
0.15	3.917	3.965	1.0122	1.64	5.80	128	240	4450	0.047	4850	0.0067	1.95	12.7	18.6
0.2	3.919	3.984	1.0165	1.60	5.79	150	225	4260	0.021	4550	0.0072	1.98	8.6	14.7
0.25	3.924	3.988	1.0163	1.55	5.78	–	190	–	–	4125	0.0088	1.82	7.1	10.7
0.3	3.934	3.994	1.0152	1.53	5.77	–	175	–	–	3775	0.0368	1.70	4.3	8.4

size may be due to the difference the ionic radius and valency of A-site cations of Bi^{3+} (131 pm) and Ba^{2+} (156 pm) which plays an important role in the grain growth mechanism. This is because beyond the solubility limit of BZT it may accumulate at the grain boundary. This would result in the inhibition of grain growth [10]. The density of the $(1-x)$BNLT$-x$BZT ceramics measured by the Archimedies method is listed in Table 1. The density of the ceramics decreased when the content of x increased.

The temperature dependence of dielectric permittivity (ε_r) and dielectric loss of the $(1-x)$BNLT$-x$BZT ceramics as a function of x at 1 kHz are shown in Fig. 5(a)–(d). For the $0.1 \le x \le 2.0$ samples, the ε_r peak exhibited two dielectric anomalies at T_p (low temperature) and T_c (high temperature) (Fig. 5(a)–(c)). The T_p is the phase transition temperature, corresponding to a ferroelectric rhombohrdral phase which transforms to a ferroelectric tetragonal phase, while, T_c is Curie temperature and relates the transition from a ferroelectric tetragonal phase to a paraelectric cubic phase [3,10]. For $x \ge 0.25$ (Fig. 5(d)), the dielectric constant curves exhibited a broad dielectric peak. The transition temperature at T_p exhibited an unclear phase transformation. The T_p increases and the T_c decreases with increasing amount of x, as shown in Table 1. The dielectric constant at T_p and T_c increased when the content of x was increased up to 0.15 and then dropped. The dielectric loss at T_p and T_c are illustrated in Table 1. The maximum dielectric constant at T_c was observed from the sintered sample with $x=0.15$. For the sample with the composition of $x=0.2$, the dielectric properties of the sample prepared by the combustion method was higher than that found using the solid-state reaction method [3]. This indicated that the combustion technique is a simple method to prepare high quality $(1-x)$BNLT$-x$BZT ceramics. The diffuseness constant (γ) which is used for explaining the diffuseness of the ferroelectric phase transition, follows a modified Curie–Weiss law [11]. The parameter γ indicates the character of the phase transition: for $\gamma=1$, a normal Curie–Weiss law and for $\gamma=2$, a complete diffuse phase transition [11]. The values of γ increased from 1.61 to 1.98 when x content increased from 0.1 to 0.2. For the sample with $x \ge 2.5$, the values of γ decreased, as shown in Table 1. Generally, the broadness or diffusiveness occurs mainly due to the change in composition and the disordered structure in the arrangement of cation in one or more crystallographic site of the structure [11]. From the compositions studied the values of γ are found to be more than 1.6. This indicates that the transitions are of a diffuse type and the materials are highly disordered [11].

The polarization (P–E) hysteresis loops of the $(1-x)$BNLT$-x$BZT ceramics with $0.1 \le x \le 0.3$ were measured at a maximum electric field of 30 kV/cm is illustrated in Fig. 6. It is evident that the shape of the P–E loops exibited a slim loop for all compositions. The remnant polarization (P_r) and the coercive field (E_c) of $(1-x)$BNLT$-x$BZT increased with the increased of x content up to 0.15. Then, they decreased with a higher content of x as shown in Table 1.

4. Conclusions

A high quality $(1-x)$BNLT–xBZT ceramic in the composition of $0.1 \le x \le 0.3$ is obtained successfully by the combustion method. The sintering temperatures and x content directly affect phase formation, microstructure and the physical properties of the ceramics. The grain size increases with increasing sintered temperatures. The highest density of ceramics was discovered in the sample sintered at 1125 °C for 2 h. The ceramics exhibited both the rhombohedral and tetragonal phases if x content ≤ 0.1 and the tetragonality increases with the increased of x content. The average gain size, the density and Curie temperature of the ceramic decrease, as the x content increasing. The phase transition from rhombohedral to tetragonal appeared in the dielectric curve where $0.1 \le x \le 0.2$. The maximum dielectric constant at Curie and the highest P_r were obtained in sample with $x=0.15$.

Acknowledgments

This work was financially supported by the Thailand Research Fund (TRF). Thanks also to Department of Physics, Faculty of Science, Naresuan University for supporting facilities. Acknowledgments to Mr. Don Hindle, for helpful comments and corrections of the manuscript.

References

[1] A. Herabut, A. Safari, Processing and electromechanical properties of $(Bi_{0.5}Na_{0.5})_{(1-1.5x)}$ La_xTiO_3 ceramics, Journal of the American Ceramic Society 80 (1997) 2954–2958.

[2] J.M. Herbert, Ferroelectric Transducers and Sensors, Gordon & Breach, New York, 1982.

[3] P. Kantha, K. Pengpat, P. Jarupoom, U. Intatha, G. Rujijanagul, T. Tunkasiri, Phase formation and electrical properties of BNLT–BZT lead-free piezoelectric ceramic system, Current Applied Physics 9 (2009) 460–466.

[4] A. Thongtha, T. Bongkarn, Optimum sintering temperature for fabrication of $0.8Bi_{0.5}Na_{0.5}TiO_3-0.2Bi_{0.5}K_{0.5}TiO_3$ lead-free ceramics by combustion technique, Key Engineering Materials 474–476 (2011) 1754–1759.

[5] A. Thongtha, T. Bongkarn, Phase formation and microstructure of barium zirconate ceramics prepared using the combustion technique, Ferroelectrics 383 (2009) 33–39.

[6] P. Panya, N. Vittayakorn, N. Phungjitt, T. Bongkarn, The structural phase and microstructure of perovskite $Ba(Ti_{1-x}Zr_x)O_3$ ceramics using the combustion route, Functional Materials Letters 2 (4) (2009) 169–174.

[7] A. Thongtha, T. Bongkarn, K. Angsukased, Fabrication of $(Ba_{1-x}Sr_x)(Zr_xTi_{1-x})O_3$ ceramics using the combustion technique, Smart Materials and Structures 19 (2010) 1–7.

[8] P. Julphunthong, T. Bongkarn, Phase formation, microstructure and dielectric properties of $Ba(Zr_{0.1}Ti_{0.9})O_3$ ceramics prepared via the combustion technique, Current Applied Physics 11 (3) (2011) 60–65.

[9] P. Sittiketkorn, A. Klinbumrung, T. Bongkarn, Influence of excess Bi_2O_3 and Na_2CO_3 on crystal structure and microstructure of bismuth sodium titanate ceramics, Key Engineering Materials 474–476 (2011) 1711–1714.

[10] K. Pengpat, S. Hanphimol, S. Eitssayeam, U. Intatha, G. Rujijanagul, T. Tunkasiri, Morphotropic phase boundary and electrical properties of lead-free bismuth sodium lanthanum titanate-barium titanate ceramics, Journal of Electroceramics 16 (2006) 301–306.

[11] S.K. Rout, E. Sinha, S. Panigrahi, Dielectric properties and diffuse phase transition in $Ba_{1-x}Mg_xTi_{0.6}Zr_{0.4}O_3$ solid solutions, Materials Chemistry and Physics 101 (2007) 428–432.